

# A comparative study of performance of heat pipes with rectangular and omega-type grooves

Valeri Vlassov, Jorge Bertoldo Junior and Nadjara dos Santos

*National Institute for Space Research, S.J.Campos-SP, Brazil*

---

## Abstract

Aluminum axial grooved heat pipes (HP) are widely used in space applications for heat spreading in the honeycomb structural panels of satellites, where electronic equipment is installed. The heat pipe grooves may be of rectangular, trapezoidal, or omega-type cross-section. The omega-type grooves usually give a better performance, however the developing capillary pressure may be sensitive to volume of fluid charge. Under ground test conditions, the HP thermal resistance may be affected by partial drying of upper grooves and eventual pool formation at the bottom area of the vapor core, especially for the heat pipes of relatively large groove size and diameter. This possible HP performance degradation must be carefully evaluated when satellite is submitted to the thermal vacuum tests. In this paper we present results of theoretical and experimental studies performed on HPs with rectangular and omega-type grooves using acetone as a working fluid. Experimental results were obtained on two similar HPs of the same external diameter but different grooves. Detailed finite element models of two types of grooves were built and simulation results were compared with obtained experimental data. Effects of partial drying and over-flooding were evaluated with the aim of a developed finite-element mathematical model of the grooves with different degrees of filling. Finally, the possible effects of using nanofluids were studied for both types of the grooves.

*Keywords:* extruded heat pipes; space applications; ground test performance; mathematical model of filled grooves

---

## 1. INTRODUCTION

Axially grooved heat pipes (HP) are widely used for the thermal stabilization of honeycomb panels of satellites. Heat pipes provide a high heat transfer rate with approximately isothermal behavior [1]. They spread the heat, dissipated by electronic equipment installed on the panel over entire panel area, avoiding the hot spots and electronic components superheating. Once the HP shall be embedded into the honeycomb panel, the best way for the insertion is when the heat pipe flanges fit the panel thickness and have the good thermal contact with the face sheets. For the panels of thickness above 20 mm, the embedded one-core ammonia heat pipe, having close external diameter, will operate very far from its capillary limits. In this situation the radial thermal resistance will be the only important parameter. Ammonia is commonly used as a working fluid in such heat pipes. Such the excess of the heat transport capability of high-diameter embedded ammonia HPs opens a possibility to use less efficient, but less hazardous and safer working fluid like acetone

One of the first theoretical and experimental studies of omega-type groove was performed in 1977 [2]; authors named this capillary structure as "covert grooves". Soon after, the term "reentrance groove" has been established and when widely used [3]. Some later, the terms "omega-shaped" or "omega-type" groove were used in parallel [11,12,14]

In general, the omega-type grooves yield a better capillary pressure and lower hydraulic losses on liquid return. In addition, as noted in [2], the retardation of the liquid flow due to the countercurrent vapor flow over the liquid-vapor interface is minimized as compared to other axial groove designs. From the other hand, these structures lead to a relatively high axial pressure drop in the liquid phase side due to an increase in the wall thickness of the heat pipe [8].

Some patents were issued where the basic configuration of the reentrant grooves were established [5, 6].

Edelstein and Kosson in 1992 [7] studied experimentally an extruded heat pipe of 24 re-entrant axial grooves in a 25.4 mm, used methane as working fluid, in cryogenic environment and also in an environment with other temperature ranges. The authors affirmed that the heat pipe offered reliability in operation and low amount of working fluid. They noted that elongated bubbles containing small concentrations of NCG can form in re-entrant groove heat pipes if the groove width is smaller than half the groove diameter.

An omega-type groove provides a large radius of curvature upon which an extended thin film of liquid phase may develop. This thin film and extended vapor-liquid interface surface allows lower thermal resistance of heat conductance from metal elements to the interface

Thomas and Damle in 2004 [8] analyzed the behavior with a re-entrant groove in laminar flow through the finite element method. The results of the numerical model were used to determine the capillary limit of a low-temperature heat pipe with two different working fluids, water and ethanol, for a range of meniscus contact angles..

In [11] authors noted that for omega-type grooves the entrainment limit is enhanced due to longer wet perimeter of wick groove and narrower slot width. However, compared with rectangular, trapezoidal, or triangular groove designs, the radial thermal resistance of "omega"- shaped groove geometry may be larger and the boiling limit might be weakened due to an increase in the wall thickness of the heat pipe.

In the present paper, the comparative study starts with elaboration of FEM numerical models of two types of the grooves: rectangular and Omega-type one. We simulated the conductive component of radial heat transfer through the groove for different meniscus configurations. Then two similar HPs of different groove types have been tested and the results were compared with the numerical simulations. The model was used to investigate the influence of thermal conductivity of the working fluid on the HTC in the evaporator and condenser zone; a possible improvement of HTC due to using of nano-fluids was also simulated.

Two heat pipes of the similar size but the different grooves, one is of rectangular and another of omega-type cross section, have been charged with acetone and then submitted to extensive performance tests. The temperature distributions along the heat pipe length have been measured under different heat loads and different temperatures of the adiabatic zone, varying from 0 C to +50C. The experimental results were compared with the results of numerical simulations.

## 2. RECTANGULAR GROOVE FEM

First the 2D models of rectangular grooves have been developed. The FEM numerical mesh of the aluminum groove filled with liquid is shown in Fig 1. In this figure, the liquid meniscus curvature matches an average heat load in the evaporator zone. Boundary conditions include heat flux input on the bottom part of the element that is a part of the HP external surface; liquid-vapor interface temperature is fixed; heat transfer between groove wall and liquid is defined through internal HTC. Other external boundaries are thermally insulated.

The present element geometry is an approximation of cylindrical HP geometry cut; we assume the difference is negligible due to very small dimension of the groove. The groove dimensions are given in Table 3.

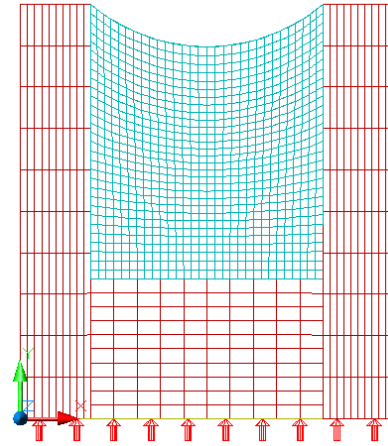


Fig. 1. An example of numerical grid of the FEM of a HP rectangular groove with meniscus.

Figure 2 shows the obtained difference temperature map over the rectangular groove in the evaporator section. Heat-load flux is  $q=3600$  W/m<sup>2</sup> and working fluid is acetone ( $k=0.181$  W/m/K at 40C). The left-side scale show the temperature increase related to vapor temperature, in C.

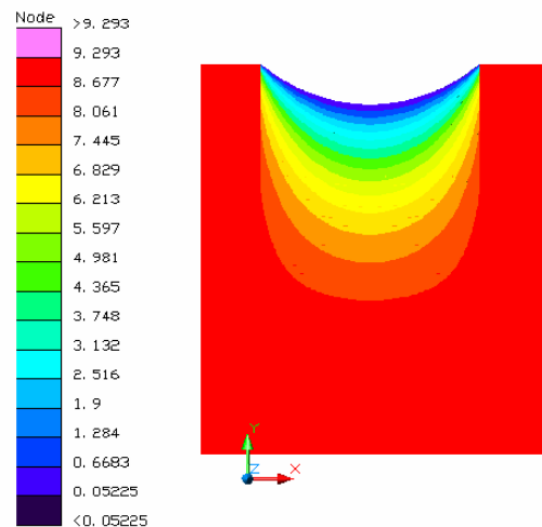


Fig. 2. Temperature distribution in the liquid meniscus of a rectangular groove.

In this simulation, heat load  $Q$  is applied from HP external surface (bottom surface in the figure). Then the heat transfer coefficient (HTC) is calculated by

$$h = \frac{Q}{\pi D_o L_{ev} (\bar{T}_w - T_{vl})} \quad (1)$$

Where  $T_w$  is the external surface-average temperature of the HP wall at evaporator (or condenser) zone and  $T_{vl}$  is the temperature on the liquid-vapor interface, measured in the middle of HP adiabatic section.

Such a HTC definition, which related to the HP external surface area, is different to that related to internal surface of liquid-vapor heat transfer and used in many other publications. Equation (1) yields lower HTC values than usual defined, however provides much more useful information to HP Users who do not care about internal HP structure and is interesting only in HP application.

By the similar way, we built various groove models with different meniscus configurations and different degrees of filling with liquid phase; see Fig 3 as an illustration.

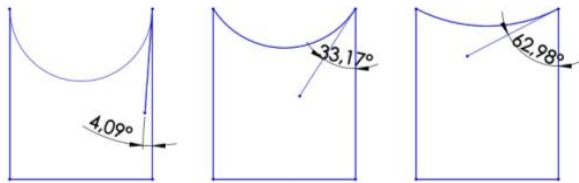


Fig. 3. Some configurations for the study referring the contact angle variations

Under high heat load, the meniscus gets deeper into the liquid bulk, the meniscus radius decreases, the overall thermal resistance between the groove wall and vapor-liquid interface also decreases, and the interface area increases. All these phenomena contribute to an increase of HTC. Figure 4 shows a simulation result how the HTC increases when the contact angle changes from 90 deg to a minimal value.

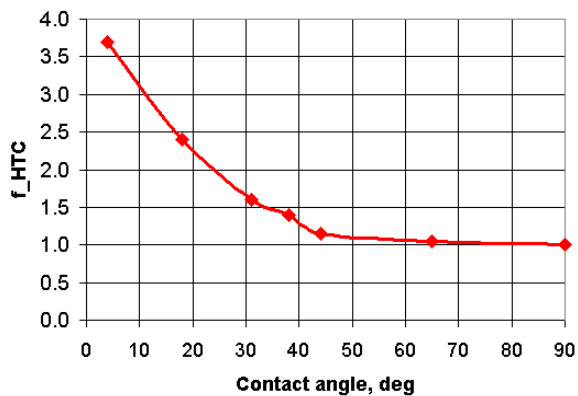


Fig. 4. Influence of contact angle developed in a rectangular groove in the evaporation zone.

Next figure show a result of numerical simulations of the influence of filling degree of groove in the condenser zone to HTC, considering plane meniscus.

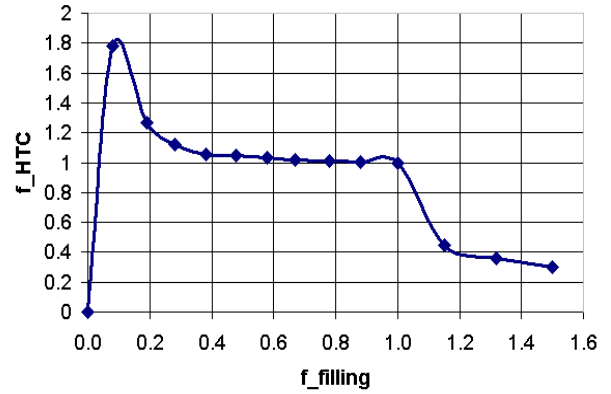


Fig. 5. Influence of filling rate of meniscus in condenser zone.

The value  $f_{filling}=1$  corresponds a plane meniscus, while  $f_{filling}>1$  relates to cases of overfilling or condenser film accumulation which can occur in the condenser zone.

The HTC depends mainly on liquid thermal conductivity. Over past decades many investigations have been performed to improve the poor thermal conductivity by using nanofluids; references [17-18] are some initial publication on this matter. Ultra-fine metallic or nonmetallic nanometer dimension particles suspended in liquid increase the conductivity and, being used in HPs, improve HTC and boiling limit.

Figure 6 shows a summary of simulation results on the study how HTC varies with liquid thermal conductivity. Factor  $f_k=1$  corresponds Acetone property (0.181 W/m/K). Different points on this graph represent some other working fluids, as well as the possible effect of nanofluids using. Table 1 describes these points. Factor HTC - is the ratio of HTC obtained for different working fluids to the HTC of pure acetone, used in the present experimental study.

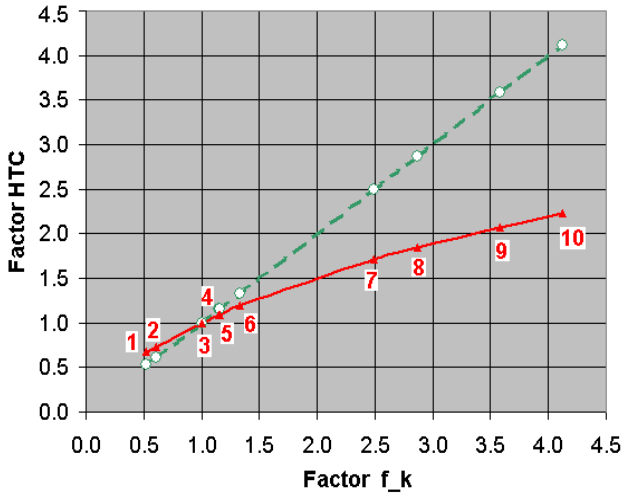


Fig. 6. Factor of HTC variation as a function of the liquid thermal conductivity.

The points are numbered from left to right and correspond following cases of the analysis (see Table 1).

Table 1. Relative HTC as a function of the liquid thermal conductivity factor.

Point	$f_k$	$f_{HTC}$	Work fluid
1	0.53	0.67	Propylen
2	0.60	0.73	Propylen+nano
3	1.00	1.00	Acetone
4	1.15	1.09	Acetone+nano
5	1.16	1.09	Methanol
6	1.33	1.19	Methanol+nano
7	2.49	1.71	Ammonia
8	2.87	1.84	Ammonia+nano
9	3.58	2.07	Water
10	4.12	2.23	Water+nano

A factor 1.15 was used here to set an improvement of liquid thermal conductivity by using nano-particles. Surely, another factor may be used to evaluate the nanofluid effect with the using of the present FEM, however all new points will match the red curve in the graph.

The graph on Fig. 6 reveals the different slopes on the curves of factors  $f_k$  and  $f_{HTC}$ . It may be interpreted by the following manner. If it would be possible to increase thermal conductivity of liquid, either by use the different working fluid or use the nano-particles, say by  $\sim 3.6$  times, the HTC improvement will be only  $\sim 2.1$  times (points 3 and 9). Therefore, the following is valid:

$$f_{HTC} \cong 0.58 f_k \quad (2)$$

Certainly, for another groove dimension, the deviation of the slops may be slightly different.

### 3. OMEGA TYPE GROOVE FEM

Figure 7 presents an amplified photo (profile measurement) of a typical omega-type HP groove.



Fig. 7. Omega-type groove amplified view (a HP profile similar to one presented in [13]).

The shape of the groove may have differences to meet performance optimization and HP user requirements.

For omega-type groove elements, different authors may use different nomenclature. In Fig 8 we present a generalized nomenclature, which was extracted from reviewed publications and completed.

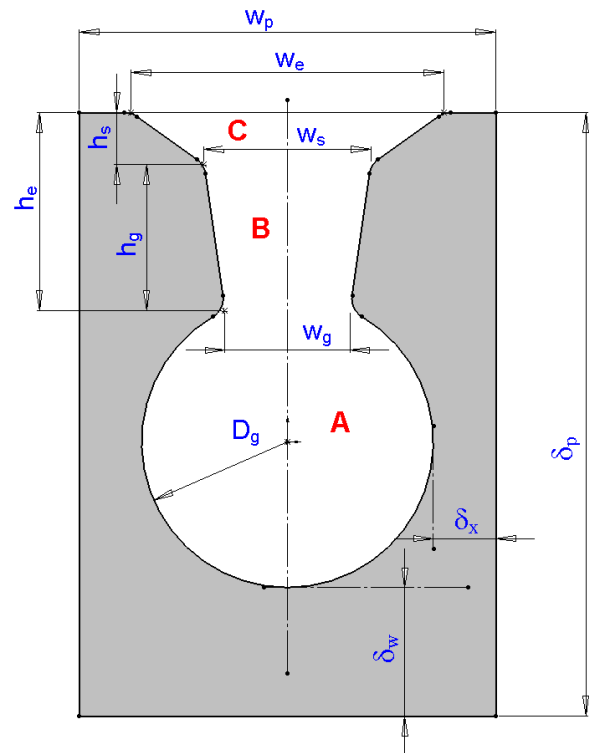


Fig. 8. Proposed parameterization of Omega-type groove.

Three regions are defined in the groove. A ("Groove") - is a groove channel, which provides a main path for liquid return, having low hydraulic losses.

B ("Gap") - is a region where the meniscus develops on evaporation. The usual attach point corresponds to  $w_s$  width, however on start-up and transients the meniscus may temporary recess into the gap bulk toward to point of  $w_g$  width. The high slope of the gap may assist on self-controlling feature, when capillary pressure increases while meniscus moves down. This slop also may contribute on eventual bubbles expulsion into the vapor channel.

C ("Slot") - is an entrance slot of low slope. The parameters of this region may be optimized by such a way that in the condenser section of HP the thermal resistance of the condensate layer will be minimal. The condensate layer design position - is a plane meniscus on the top of the C-region; the low slope yields small liquid equivalent thickness and small thermal resistance from aluminum rib surface to the liquid-vapor interface.

The nomenclature is given in Table 2, where some values of the key parameters of Omega-grooves are given as examples.

Table 2. Main parameters of some omega-groove profiles.

Par	Name / Dim (mm)	HP[2]	HP[16]	HP[13]
$D_0$	Outer HP diameter	12.7	17	20
$D_g$	Diameter of groove	0.8	1.35	1.3
$h_e$	Height of entrance	0.25	1.0	1.2
$h_s$	Height of slot	0		0.5
$h_g$	Height of gap	0.25		0.65
$w_e$	Width of entrance	0.27		1.45
$w_s$	Width of slot	0.27		0.5
$w_g$	Width of groove opening	0.22	0.65	0.4
$\delta_p$	groove element thickness	1.7	4.2	3.4
$\delta_w$	HP wall thickness	0.64	1.8	1.2
$\delta_x$	Extrusion limit thickness	N/A		0.6

In the evaporator zone under nominal operation the meniscus shall be located in the zone B. The FEM model, shown in Fig. 9, simulates such a configuration.

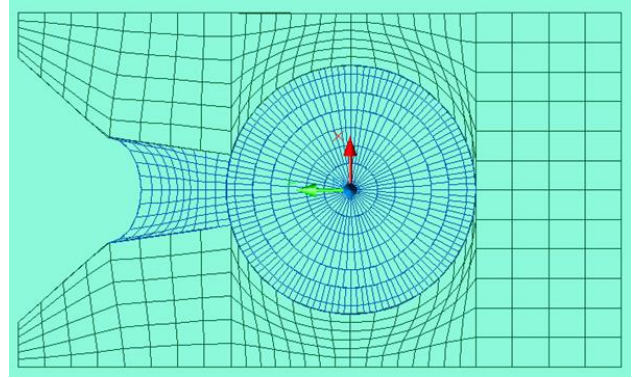


Fig. 9. Proposed numerical grid for omega-type groove FEM in evaporation zone (rotated 90 deg)

The FEM model allows simulation the conductive radial component of HTC. Due to very small size and low velocities, the convective component contribution is relatively low, in the order of about ~30-50 %. In the Test Results section this factor is evaluated by comparison with the obtained experimental data.

Figure 10 shows the distribution of temperature differences over the interface temperature for the evaporation HP zone. The input data are the same as for rectangular groove (Fig. 2).

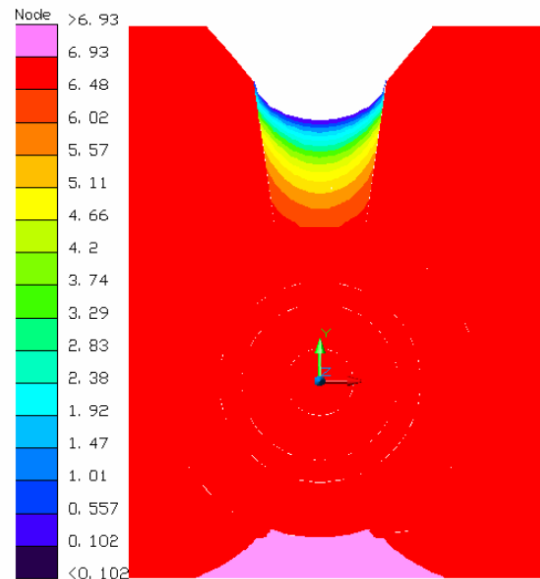


Fig. 10. Temperature difference map in a groove filled with liquid in the evaporation zone.

Next Figures demonstrate separately the temperature gradients developed in the metal part of the groove (Fig 11) and in the gap region (Fig. 12). The gradients in the aluminum are limited of about 0.1 C, while the principal gradients, as expected, develop into the liquid gap region.

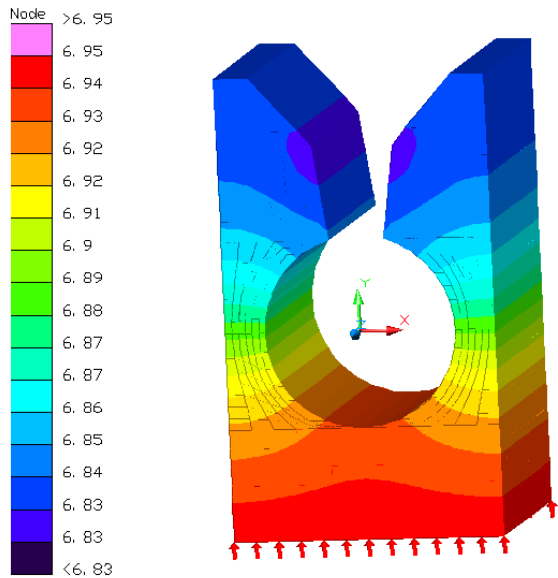


Fig. 11. Temperature gradients developed in the metallic elements of the groove.

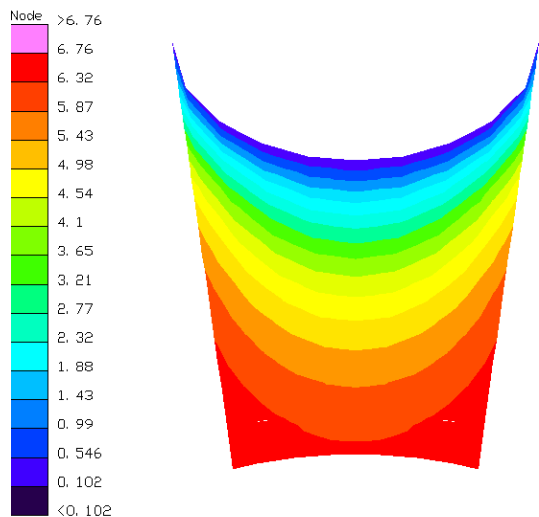


Fig. 12. Temperature gradients developed in the gap region.

Temperature radial gradients in the liquid groove are very small (Fig.14), because the principal heat transfer takes place in the meniscus region.

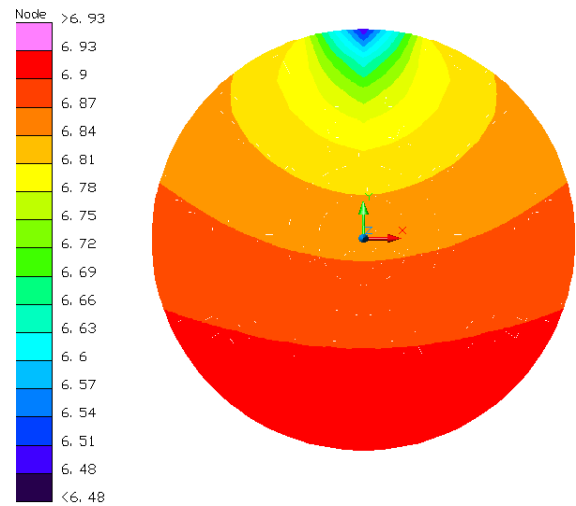


Fig. 13. Temperature gradients in liquid in the groove.

The groove in the condenser section is simulated having the different expected meniscus configuration; the corresponding numerical grid is shown in Fig. 14.

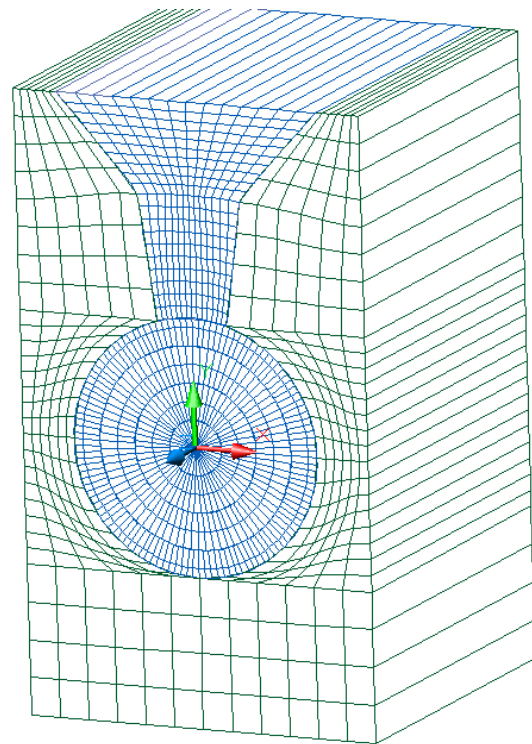


Fig. 14. Numerical grid for omega-type groove FEM in evaporation zone (rotated 90 deg)

Figure 15 shows the map of temperature differences below the liquid-vapor interface temperature over the omega-groove in the condenser HP zone.

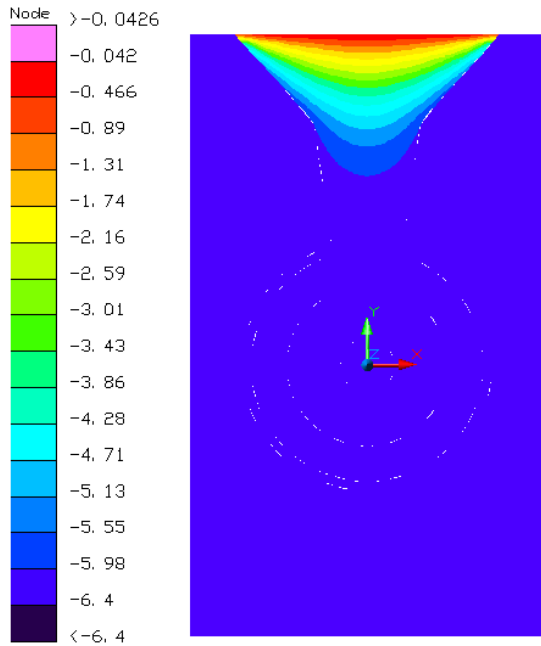


Fig. 15. Temperature difference map in a groove filled with liquid in the condenser zone.

In general, compared to temperature distribution of the rectangular groove, the omega-type groove does not yield a radial HTC decrease because of relatively high of groove element thickness  $\delta_p$ , as it noted in some publications [8]. The primary heat transfer takes place near meniscus and temperature gradients in other elements of the groove structure are minimal. The HTC depends essentially on the meniscus curvature and the slot width (or the groove width in the case of rectangular configuration).

#### 4. TEST SETUP

Two heat pipes of the similar size but the different grooves have been charged with acetone and then submitted to extensive performance tests. One HP is of rectangular and another is of omega-type cross section; main HP dimensions are given in Table 3.

Table 3. Main dimension of experimental HPs.

	HP rectangular	HP omega
HP length, mm	730	640
Diameter ( $D_0$ ), mm	18.4	19.6
Dv - vapor channel diameter	12.4	11.8
Lev - evaporator length, mm	205	205
Lcond - condenser length	175	175
N of grooves	24	27
w <sub>s</sub> - width of slot/groove, mm	1.3	0.52
Work fluid	Acetone	Acetone

. The temperature distributions along the heat pipe length were measured under different heat loads, varying from 15W to 60W, and different temperatures of the adiabatic zone, varying from 0° C to +50° C.

A styrofoam insulates the HP from ambient temperature; and a foam insulates the coolant system lines. Heat is applied to one HP end symmetrically from lateral surfaces with two skin electrical heater of 207 mm x 19 mm. Heat is removed from the opposite HP end by a coolant circuit of a thermostat, which controls the coolant temperature from -30° C to + 100° C with the precision of  $\pm 1^\circ$  C. Total 58 type-T thermocouples are installed throughout the each tube as shown in Fig.16.

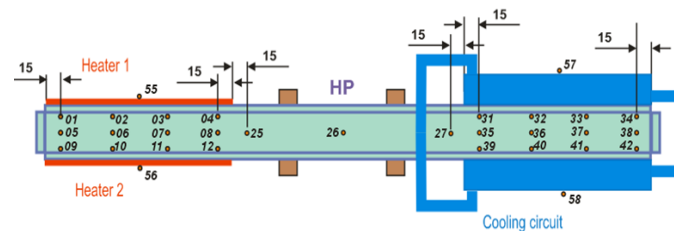


Fig. 16. HP themocouple positions (one side).

The two heat pipes is fixed firmly through insulation supports on the table, see Fig. 17.



Fig. 17. Both heat pipes installed on the table.

The horizontal leveling is controlled with a digital precise inclinometer with a sensitivity of  $\pm 0.01$  degrees.

#### 5. TEST RESULTS AND COMPARISON

Next figures shows experimental steady-state temperature profiles obtained under different heat dissipations varying from 15 to 60 W. The temperature profiles in Fig. 18 are plotted for the HP with rectangular grooves for the adiabatic section temperature of +40 C.

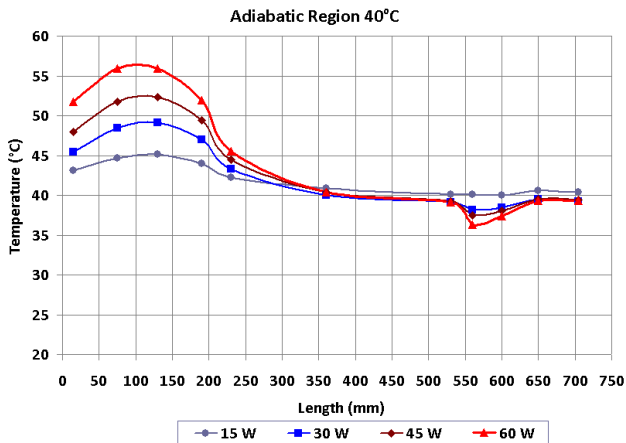


Fig. 18. Steady-state temperature profile of acetone HP with rectangular grooves.

The HP with rectangular grooves presented some temperature anomalies at the entrance of the condenser zone and at the central part of evaporator. The groove width is relatively high, and the surface tension is not enough to keep liquid in upper grooves - they may be partially dried. However, at the begin of the evaporation zone, there is a liquid communication of upper groove with bottom groove either through a technology gap or through an eventual liquid slug trapped in the vapor channel at the end cup proximity. Therefore, the temperature measured by TC01 thermocouple is lower than TC02-TC04 of the evaporation zone.

Liquid drained from upper grooves for a puddle at the HP bottom. Acetone vapor flows with a relatively high velocity drives this liquid excess toward the condenser zone, where it accumulates and, together with vapor condensation process, forms a local liquid film of relatively high thickness. In this position HTC gets a decrease and the HP wall temperature replies with a slight local decrease, differently to other condenser temperatures. Such an effect repeats at other vapor temperatures.

The omega-type grooves yield a better total thermal resistance in the evaporator zone than the rectangular grooves, as shown in Fig 17.

At begin of the evaporator zone, one can observe the similar temperature profile behavior. However, at the condenser zone such a liquid film accumulation, observed in the rectangular grooves, does not take place in the omega-grooves. It can be explained by a function of the groove slot (region C in Fig 8), which prevent such an accumulation. However, there are signals that in this case the liquid excess forms a slug at the end of the condenser zone.

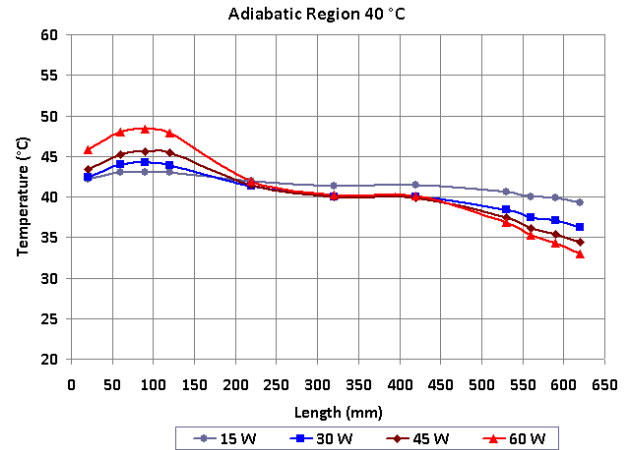


Fig. 19. Comparative temperature profile of the similar heat pipe with omega-type grooves.

Experimental data was compared with simulation results for the same case of 45W heat load and 40 C of vapor temperature. The results for experimental and numerically obtained values of HTC are given in Table 4 separately for evaporator and condenser zones.

Table 4. Numerical and experimental results.

[W/m <sup>2</sup> /K]	HTC_exp	HTC_num
Omega_ev	696	736
Omega_cond	784	622
Rectangular_ev	330	405
Rectangular_cond	2883	--

The HTC is defined through the external HP area and temperature difference between external surface and vapor temperature for acetone, in accordance to Eq. 1.

The differences between the experimental and simulation results lie within 5% to 26% and can be explained by several phenomena, which were not considered in the mathematical model:

- 1) Convective component of in-groove heat transfer
- 2) Uncertainty in definition of a real meniscus curvature.
- 3) Effects of partial grooves drying and flooding of some grooves

Figure 20 shows a summary of simulation results on the study how HTC varies with liquid thermal conductivity for the omega-type grooves. The points on this graph represent some other working fluids, as well as the possible effect of nanofluids using. Table 1 describes these points; they are the same as for rectangular grooves, however the values of the Factor HTC are slightly different.

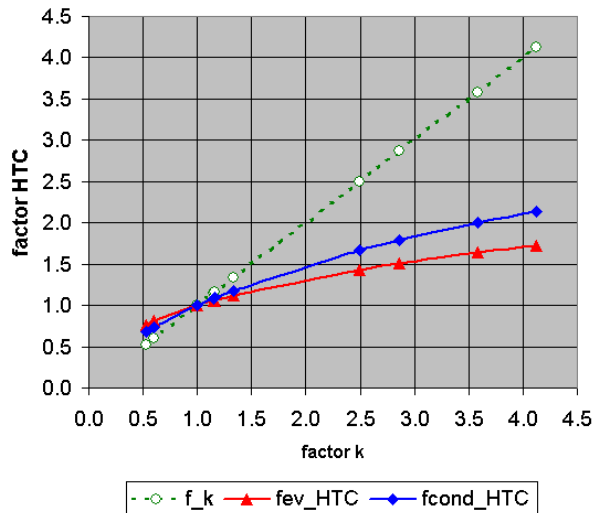


Fig. 20. HTC Factor variation as a function of liquid thermal conductivity.

The average slopes of the Factor HTC are the following, for the evaporator and condenser zones correspondingly:

$$f_{HTC,ev} \cong 0.46f_k \quad f_{HTC,cond} \cong 0.56f_k \quad (3)$$

The slope of the evaporator curve (0.46) for the omega-type groove is about 20% lesser than for the case of the rectangular groove. It means the specific omega-shaped configuration makes such type a groove slightly less sensitive to the liquid thermal conductivity property.

## 6. CONCLUSIONS

Theoretical and experimental studies were performed on HPs with rectangular and omega-type grooves using acetone as a working fluid. Experimental results were obtained on two similar HPs of the same external diameter but different grooves. Detailed FEM models of two types of grooves were built and simulation results were compared with experimental data. The deviations in HTC values were explained. The following conclusion can be derived.

The radial thermal resistance to heat transfer of the omega-groove geometry did not present any reduction compared to rectangular grooves, in spite of an increase in the wall thickness of the HP

2D FEM conduction models of grooves with different degrees of liquid filling represented overall radial heat transfer within 26 % of uncertainty confirmed by experimental data.

Variation of contact angle may yields of HTC variations up to 3.7 times. Any effects of overflowing in the condenser zone may drop the HTC up to 3 times.

Both rectangular and omega grooves presented a similar behavior in the evaporator zone, but the HTC of the rectangular groove was almost twice lower.

The behavior in the condenser zone of both HPs is more complicated. A superposition of the effects of excess liquid entrainment and high vapor velocity stagnation (that is the characteristic of low-pressure fluids like acetone) makes it difficult to evaluate HTC in the condenser due to uncertainty of liquid puddle configuration, especially for rectangular grooves.

The present approach with FEM allows evaluating the effect of using nanofluids to the HTC value improvement. A reduction factor of 0.46 to 0.58 shall be applied to evaluate the HTC increasing when the liquid thermal conductivity increase by using of nanoparticles. Rectangular grooves have a slightly higher sensitivity to nanofluid using.

## ACKNOWLEDGEMENT

Authors acknowledge the CNPq organization grant 311347/2015 and CAPES grant 1456650/PNPD for the support of the present research

## NOMENCLATURE

- $q$  : Heat flux (W/m<sup>2</sup>)
- $HTC$  : Heat Transfer Coefficient (W/m<sup>2</sup>/K)
- $HP$  : Heat Pipe
- $FEM$  : Finite Element Model
- $FE$  : Finite Element
- $N/A$  : not available
- $h$  : Heat Transfer Coefficient (W/m<sup>2</sup>/K)
- $T$  : Temperature (K)

## REFERENCES

- [1] Grover, G.M., Cotter, T. P., Erickson, G.F., Structures of very high thermal conductance. *Journal of Applied Physics*, 35(6) (1964) 1990- 1991.
- [2] Kaufman, W. B., Tower, L. K., Analysis and tests of NASA covert groove heat pipe. NASA CR-135156 Report, Grumman AC (1976) 55p.
- [3] Harwell, W., Kaufman, W. B., and Tower, L. K., Re-Entrant Groove Heat Pipe, Proc. *12th AIAA Thermophysics Conference*, 77-773 (1977) 131-147.
- [4] Schlitt, K.R., Brennan, P.J. Kirkpatrick, J.P., Parametric performance of Extruded Axial grooved Heat Pipes from 100 to 300 K, *Heat Transfer with thermal Control Applications*, 39 (1975) 215-227.
- [5] Joseph P. Alario, Robert L. Kosson, Edward Leszak. Re-entrant groove heat pipe. *US Patent* 4 545 427-1985
- [6] Fred Edelstein and Robert L. Kosson. Large capacity

re-entrant groove heat pipe. *US Patent 5 219 021-1991*

- [7] Edelstein, F., Kosson, R. L., A high capacity re-entrant groove heat pipe for cryogenic and room temperature. Grumman AC, *Cryogenics*, 32 (1992) 167-172.
- [8] Scott, K. T., Damle, V.C., Analysis of Fluid Flow in Axial Re-entrant Grooves with Application to Heat Pipes. *AIAA Thermophysics Conference*, 2177 (2004).
- [9] Schlitt, R., Performance Characteristics of Recently Developed High-Performance Heat Pipes, *Heat Transfer Engineering*, 16 (1) (1995) 44-52.
- [10] Vlassov, V.V., Transient Model of a Grooved Heat Pipe Embedded in the Honeycomb Structural Panel. *35th International Conference on Environmental Systems*, Rome, Italy, (2005) 14 pp.
- [11] Chen, Y., Zhang, C., Shi, M., Wu, J., Peterson, G.P., Study on flow and heat transfer characteristics of heat pipe with axial “ $\Omega$ ”-shaped microgrooves. *International Journal of Heat and Mass Transfer* 52 (2009) 636-643.
- [12] Chen, Y., Yao, F., Shi, M., Thermal response of a heat pipe with axially “ $\Omega$ ”-shaped microgrooves. *International Journal of Heat and Mass Transfer* 55 (2012) 4476-4484.
- [13] Shibano, Y., Ogawa, H., Thermal performance of re-entrant groove heat pipe: dependence on orientation and temperature. *Heat Pipe Science and Technology, An International Journal* 5 (1-4) (2014) 237-243.
- [14] Goncharov, K., Antonov, V., Vinokurov, Y., Experience of space application of axial groove heat pipes with  $\Omega$ -shape grooves. *Heat Pipe Science and Technology, An International Journal* 5 (1-4) (2014) 571-578.
- [15] Shibano, Y., Ogawa, H., Thermal behavior of axial groove heat pipe under gravity: dependence of groove shape and orientation. *45th International Conference on Environmental Systems*, Bellevue, Washington, USA (2015) 126.
- [16] Pismennyi, E.N., Khairnasov, S.M., Rassamakin, B.M., Heat Transfer in Evaporation Zone of Ammonia Aluminium Heat Pipes. DOI: 10.20535/1810-0546.2017.1.82925 (2017) 10p
- [17] D.B. Tuckerman, R.F. Pease, High-performance heat sinking for VLSI, *IEEE Electron. Dev. Lett.* EDL-2 (1981) 126–129.
- [18] Choi, U.S., 1995. Enhancing thermal conductivity of fluids with nanoparticles. *ASME FED* 231, 99-103.